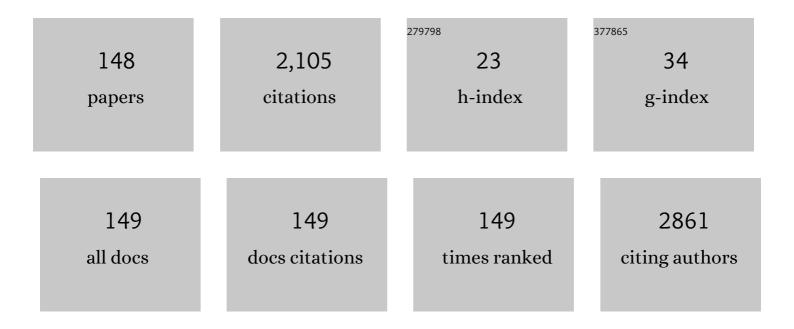
List of Publications by Year in descending order

Source: https://exaly.com/author-pdf/4538784/publications.pdf Version: 2024-02-01



#	Article	IF	CITATIONS
1	The inclusion of ceramic carbides dispersion in In and Yb filled CoSb3 and their effect on the thermoelectric performance. Journal of Alloys and Compounds, 2022, 893, 162400.	5.5	8
2	Monodispersed nanoplatelets of samarium oxides for biosensing applications in biological fluids. Electrochimica Acta, 2022, 402, 139532.	5.2	2
3	Growth and characterization of 3.5 at.% Nd:LGSB bifunctional crystal. Optical Materials, 2022, 123, 111832.	3.6	3
4	Microwave and Terahertz Properties of Spark-Plasma-Sintered Zr0.8Sn0.2TiO4 Ceramics. Materials, 2022, 15, 1258.	2.9	3
5	Effect of chlorine and bromine on the perovskite crystal growth in mesoscopic heterojunction photovoltaic device. Materials Science in Semiconductor Processing, 2022, 143, 106558.	4.0	4
6	Investigations Regarding the Addition of ZnO and Li2O-TiO2 to Phosphate-Tellurite Glasses: Structural, Chemical, and Mechanical Properties. Materials, 2022, 15, 1644.	2.9	0
7	Bulk and surface characteristics of co-electrodeposited Cu2FeSnS4 thin films sulfurized at different annealing temperatures. Journal of Alloys and Compounds, 2022, 906, 164379.	5.5	8
8	Charge transport mechanisms in free-standing devices with electrospun electrodes. Nanotechnology, 2022, 33, 395203.	2.6	4
9	Pulsed Laser Deposition Films Based on CdSe-Doped Zinc Aluminophosphate Glass. Jom, 2021, 73, 495-503.	1.9	5
10	Effect of starting materials and sintering temperature on microstructure and optical properties of Y2O3:Yb3+ 5 at% transparent ceramics. Journal of Advanced Ceramics, 2021, 10, 49-61.	17.4	39
11	Intrinsic Dielectric Loss in Zr0.8Sn0.2TiO4 Ceramics Investigated by Terahertz Time Domain Spectroscopy. Materials, 2021, 14, 216.	2.9	4
12	Structural, morphological and optical properties of Cu–Fe–Sn–S thin films prepared by electrodeposition at fixed applied potential. Thin Solid Films, 2021, 721, 138547.	1.8	11
13	Antibacterial composite coatings of MgB2 powders embedded in PVP matrix. Scientific Reports, 2021, 11, 9591.	3.3	11
14	MgB2 powders and bioevaluation of their interaction with planktonic microbes, biofilms, and tumor cells. Journal of Materials Research and Technology, 2021, 12, 2168-2184.	5.8	10
15	Fabrication of ZnO and TiO2 Nanotubes via Flexible Electro-Spun Nanofibers for Photocatalytic Applications. Nanomaterials, 2021, 11, 1305.	4.1	15
16	Redox Mechanism of Azathioprine and Its Interaction with DNA. International Journal of Molecular Sciences, 2021, 22, 6805.	4.1	4
17	Influences of Dispersions' Shapes and Processing in Magnetic Field on Thermal Conductibility of PDMS–Fe3O4 Composites. Materials, 2021, 14, 3696.	2.9	3
18	The Physico-Chemical Properties and Exploratory Real-Time Cell Analysis of Hydroxyapatite Nanopowders Substituted with Ce, Mg, Sr, and Zn (0.5–5 at.%). Materials, 2021, 14, 3808.	2.9	9

#	Article	IF	CITATIONS
19	Magnetic and Magnetostrictive Properties of Ni50Mn20Ga27Cu3 Rapidly Quenched Ribbons. Materials, 2021, 14, 5126.	2.9	1
20	Secondary phases and their influence on optical and electrical properties of electrodeposited Cu2FeSnS4 films. Applied Physics A: Materials Science and Processing, 2021, 127, 1.	2.3	6
21	Multifunctional GaFeO3 Obtained via Mechanochemical Activation Followed by Calcination of Equimolar Nano-System Ga2O3–Fe2O3. Nanomaterials, 2021, 11, 57.	4.1	2
22	Biomorphic 3D fibrous networks based on ZnO, CuO and ZnO–CuO composite nanostructures prepared from eggshell membranes. Materials Chemistry and Physics, 2020, 240, 122205.	4.0	21
23	Reticulated Mesoporous TiO ₂ Scaffold, Fabricated by Spray Coating, for Largeâ€Area Perovskite Solar Cells. Energy Technology, 2020, 8, 1900922.	3.8	19
24	Synthesis of Core–Double Shell Nylon-ZnO/Polypyrrole Electrospun Nanofibers. Nanomaterials, 2020, 10, 2241.	4.1	7
25	Graphene Oxide Concentration Effect on the Optoelectronic Properties of ZnO/GO Nanocomposites. Nanomaterials, 2020, 10, 1532.	4.1	33
26	Novel Ecogenic Plasmonic Biohybrids as Multifunctional Bioactive Coatings. Coatings, 2020, 10, 659.	2.6	10
27	Performant Composite Materials Based on Oxide Semiconductors and Metallic Nanoparticles Generated from Cloves and Mandarin Peel Extracts. Nanomaterials, 2020, 10, 2146.	4.1	7
28	Magneto-functionalities of La1-xAxMnO3 (AÂ= K; Ba) synthesized by flash combustion method. Journal of Alloys and Compounds, 2020, 839, 155546.	5.5	7
29	Cytotoxicity, Antioxidant, Antibacterial, and Photocatalytic Activities of ZnO–CdS Powders. Materials, 2020, 13, 182.	2.9	14
30	Control of the Critical Current Density Through Microstructural Design by Ho2O3 and Te Co-addition into MgB2 Processed by Ex Situ Spark Plasma Sintering. , 2020, , 303-324.		2
31	Adsorption, wicking behavior and photodegradation tests of Rhodamine B solution upon wool substrates. , 2020, , .		1
32	PCL-ZnO/TiO2/HAp Electrospun Composite Fibers with Applications in Tissue Engineering. Polymers, 2019, 11, 1793.	4.5	11
33	Thermophysical and mechanical properties of W-Cu laminates produced by FAST joining. Fusion Engineering and Design, 2019, 146, 2371-2374.	1.9	10
34	Nanostructured palladium doped nickel electrodes for immobilization of oxidases through nickel nanoparticles. Electrochimica Acta, 2019, 315, 102-113.	5.2	12
35	Spectroscopic investigations of Pr3+ ions doped CNGG and CLNGG single crystals. Journal of Alloys and Compounds, 2019, 799, 288-301.	5.5	8
36	Development of W-monoblock divertor components with embedded thermal barrier interfaces. Fusion Engineering and Design, 2019, 146, 1351-1354.	1.9	3

#	Article	IF	CITATIONS
37	Prototype Orthopedic Bone Plates 3D Printed by Laser Melting Deposition. Materials, 2019, 12, 906.	2.9	21
38	Effect of high gamma radiations on physical properties of In2S3 thin films grown by chemical bath deposition for buffer layer applications. Results in Physics, 2019, 13, 102115.	4.1	17
39	Physical properties investigation of samarium doped calcium sulfate thin films under high gamma irradiations for space photovoltaic and dosimetric applications. Superlattices and Microstructures, 2019, 126, 103-119.	3.1	5
40	Highly transparent Yb:Y2O3 ceramics obtained by solid-state reaction and combined sintering procedures. Ceramics International, 2019, 45, 3217-3222.	4.8	17
41	Magneto-optical properties of Ce3+ and Tb3+-doped silico-phosphate sol-gel thin films. Applied Surface Science, 2018, 448, 474-480.	6.1	4
42	High temperature thermo-physical properties of SPS-ed W–Cu functional gradient materials. Materials Research Express, 2018, 5, 026502.	1.6	9
43	Yellow laser potential of cubic Ca3(Nb,Ga)5O12:Dy3+ and Ca3(Li,Nb,Ga)5O12:Dy3+ single crystals. Journal of Alloys and Compounds, 2018, 739, 806-816.	5.5	16
44	Physical-chemical characterization and biological assessment of simple and lithium-doped biological-derived hydroxyapatite thin films for a new generation of metallic implants. Applied Surface Science, 2018, 439, 724-735.	6.1	32
45	Thermophysical properties of Cu-ZrO2 composites as potential thermal barrier materials for a DEMO W-monoblock divertor. Fusion Engineering and Design, 2018, 127, 179-184.	1.9	11
46	A Comparative Study of Ge-Based Organometallic Additions to MgB ₂ . IEEE Transactions on Applied Superconductivity, 2018, 28, 1-5.	1.7	4
47	Dense Ge nanocrystals embedded in TiO2 with exponentially increased photoconduction by field effect. Scientific Reports, 2018, 8, 4898.	3.3	32
48	1532â€nm sensitized luminescence and up-conversion in Yb,Er:YAG transparent ceramics. Optical Materials, 2018, 77, 221-225.	3.6	6
49	Compressive properties of pristine and SiC-Te-added MgB 2 powders, green compacts and spark-plasma-sintered bulks. Ceramics International, 2018, 44, 10181-10191.	4.8	17
50	Photocatalytic activity of wool fabrics deposited at low temperature with ZnO or TiO2 nanoparticles: Methylene blue degradation as a test reaction. Catalysis Today, 2018, 306, 251-259.	4.4	43
51	Effect of green body annealing on laser performance of YAG:Nd3+ ceramics. Ceramics International, 2018, 44, 4487-4490.	4.8	4
52	Wet chemical synthesis of ZnO-CdS composites and their photocatalytic activity. Materials Research Bulletin, 2018, 99, 174-181.	5.2	46
53	Dwell Time Influence on Spark Plasma-Sintered MgB2. Journal of Superconductivity and Novel Magnetism, 2018, 31, 317-325.	1.8	21
54	(Fe, Nd) codoped ZnO micro– and nanostructures with multifunctional characteristics like photocatalytic activity, optical and ferromagnetic properties. Ceramics International, 2018, 44, 21962-21975.	4.8	11

#	Article	IF	CITATIONS
55	Effects of a surfactant on the morphology and photocatalytic properties of polycrystalline Fe-doped ZnO powders. Journal of Physics and Chemistry of Solids, 2018, 121, 319-328.	4.0	10
56	Hierarchical functionalization of electrospun fibers by electrodeposition of zinc oxide nanostructures. Applied Surface Science, 2018, 458, 555-563.	6.1	13
57	Annealing-Induced High Ordering and Coercivity in Novel L10 CoPt-Based Nanocomposite Magnets. Metals, 2018, 8, 466.	2.3	6
58	White-Light Emission of Dye-Doped Polymer Submicronic Fibers Produced by Electrospinning. Polymers, 2018, 10, 737.	4.5	5
59	Enhanced near-infrared response of a silicon solar cell by using an up-conversion phosphor film of Yb/Er – co-doped CeO2. Solar Energy, 2018, 171, 40-46.	6.1	7
60	Effect of mixing complexing agents on the properties of electrodeposited CZTS thin films. Optical Materials, 2018, 83, 252-256.	3.6	28
61	Optical properties of Sm 3+ doped Ca 3 (Nb,Ga) 5 O 12 and Ca 3 (Li,Nb,Ga) 5 O 12 single crystals. Journal of Luminescence, 2017, 186, 175-182.	3.1	17
62	Cu-based composites as thermal barrier materials in DEMO divertor components. Fusion Engineering and Design, 2017, 124, 1131-1134.	1.9	12
63	Production of 82Se enriched Zinc Selenide (ZnSe) crystals for the study of neutrinoless double beta decay. Journal of Crystal Growth, 2017, 475, 158-170.	1.5	41
64	From an Anomalous Peak Effect to a Second Magnetization Peak in Nb-rich Nb-Ti Alloys. Journal of Superconductivity and Novel Magnetism, 2017, 30, 1103-1108.	1.8	1
65	Caspase-8, association with Alzheimer's Disease and functional analysis of rare variants. PLoS ONE, 2017, 12, e0185777.	2.5	38
66	Tellurium addition as a solution to improve compactness of <i>ex-situ</i> processed MgB ₂ -SiC superconducting tapes. Superconductor Science and Technology, 2016, 29, 065012.	3.5	8
67	Spark plasma sintered MgB 2 co-added with c-BN and C 60. Materials Chemistry and Physics, 2016, 170, 201-209.	4.0	10
68	Interfacial mechanisms of novel laser-irradiated L10-based nanocomposite magnets. Applied Physics A: Materials Science and Processing, 2016, 122, 1.	2.3	1
69	Association between ultrasonographic parameters of Cesarean scar defect and outcome of early termination of pregnancy. Ultrasound in Obstetrics and Gynecology, 2016, 47, 506-510.	1.7	7
70	Physical Properties of Polycrystalline CuGeO3 Prepared by Field-assisted Sintering Technique. Journal of Superconductivity and Novel Magnetism, 2016, 29, 775-780.	1.8	1
71	Influence of metallic and semiconducting nanostructures on the optical properties of dye-doped polymer thin films. Thin Solid Films, 2016, 614, 31-35.	1.8	7
72	CdS quantum dots sensitized TiO2 nanotubes by matrix assisted pulsed laser evaporation method. Ceramics International, 2016, 42, 9011-9017.	4.8	9

#	Article	lF	CITATIONS
73	Electrical properties of templateless electrodeposited ZnO nanowires. Materials Science in Semiconductor Processing, 2016, 42, 364-372.	4.0	13
74	Enhancing antimicrobial activity of TiO2/Ti by torularhodin bioinspired surface modification. Bioelectrochemistry, 2016, 107, 14-24.	4.6	55
75	Effect of polyhedral oligomeric silsesquioxane nanoreinforcement on the properties of epoxy resin/monoglycidylether-terminated poly(dimethylsiloxane) nanocomposites. High Performance Polymers, 2016, 28, 724-734.	1.8	3
76	Fabrication of magnetite-based core–shell coated nanoparticles with antibacterial properties. Biofabrication, 2015, 7, 015014.	7.1	25
77	Exciton-phonon interaction in PbI2 revealed by Raman and photoluminescence studies using excitation light overlapping the fundamental absorption edge. Materials Research Bulletin, 2015, 70, 762-772.	5.2	25
78	B4C in ex-situ spark plasma sintered MgB2. Current Applied Physics, 2015, 15, 1262-1270.	2.4	8
79	The influence of heating rate on superconducting characteristics of MgB2 obtained by spark plasma sintering technique. Physica C: Superconductivity and Its Applications, 2015, 519, 184-189.	1.2	13
80	Novel nanocomposites based on epoxy resin/epoxy-functionalized polydimethylsiloxane reinforced with POSS. Composites Part B: Engineering, 2015, 75, 226-234.	12.0	60
81	Ge-Added MgB2 Superconductor Obtained by Ex Situ Spark Plasma Sintering. Journal of Superconductivity and Novel Magnetism, 2015, 28, 531-534.	1.8	6
82	Microbial colonization of biopolymeric thin films containing natural compounds and antibiotics fabricated by MAPLE. Applied Surface Science, 2015, 336, 234-239.	6.1	9
83	Superior biofunctionality of dental implant fixtures uniformly coated with durable bioglass films by magnetron sputtering. Journal of the Mechanical Behavior of Biomedical Materials, 2015, 51, 313-327.	3.1	36
84	Effect of thermal treatments on the structural and magnetic transitions in melt-spun Ni-Fe-Ga-(Co) ribbons. Journal of Alloys and Compounds, 2015, 650, 664-670.	5.5	21
85	Zinc oxide electroless deposition on electrospun PMMA fiber mats. Materials Letters, 2015, 138, 238-242.	2.6	17
86	Metallic Nanowires and Nanotubes Prepared by Template Replication. Springer Series in Materials Science, 2014, , 137-165.	0.6	1
87	Physical properties of Al <i>x</i> In1â^' <i>x</i> N thin film alloys sputtered at low temperature. Journal of Applied Physics, 2014, 116, .	2.5	18
88	Indium–tin nanoscaled oxides synthesized under hydrothermal supercritical and postannealing pathway: Phase dynamics and characterization. Materials Chemistry and Physics, 2014, 143, 1540-1549.	4.0	6
89	Polysaccharide-assisted crystallization of ZnO micro/nanostructures. Materials Letters, 2014, 115, 256-260.	2.6	21
90	Micropatterned ZnO rod arrays prepared by Auâ€catalyzed electroless deposition. Physica Status Solidi - Rapid Research Letters, 2014, 8, 648-652.	2.4	4

#	Article	IF	CITATIONS
91	Influence of morphology on the emissive properties of dye-doped PVP nanofibers produced by electrospinning. Journal of Physics and Chemistry of Solids, 2014, 75, 1365-1371.	4.0	16
92	Significant enhancement of the critical current density for cubic BN addition into <i>ex situ</i> spark plasma sintered MgB ₂ . Superconductor Science and Technology, 2014, 27, 095013.	3.5	23
93	Superhydrophobic ZnO networks with high water adhesion. Nanoscale Research Letters, 2014, 9, 385.	5.7	23
94	Addition of Ho2O3 of different types to MgB2 in the ex-situ Spark Plasma Sintering: Simultaneous control of the critical current density at low and high magnetic fields. Materials Chemistry and Physics, 2014, 146, 313-323.	4.0	15
95	High magnetic field enhancement of the critical current density by Ge, GeO2 and Ge2C6H10O7 additions to MgB2. Scripta Materialia, 2014, 82, 61-64.	5.2	22
96	Cell Adhesion Response on Femtosecond Laser Initiated Liquid Assisted Silicon Surface. Current Topics in Medicinal Chemistry, 2014, 14, 624-629.	2.1	2
97	Zinc Oxide and Polysaccharides: Promising Candidates for Functional Nanomaterials. Springer Series in Materials Science, 2014, , 109-136.	0.6	1
98	Silicon bump arrays by near-field enhanced femtosecond laser irradiation in fluorine liquid precursors. Applied Surface Science, 2013, 278, 301-304.	6.1	5
99	Single bath electrodeposition of samarium oxide/zinc oxide nanostructured films with intense, broad luminescence. Electrochimica Acta, 2013, 95, 170-178.	5.2	4
100	Functionalized magnetite silica thin films fabricated by MAPLE with antibiofilm properties. Biofabrication, 2013, 5, 015007.	7.1	36
101	Periodic arrays of nanostructures in silicon and gallium arsenide by near-field enhanced laser irradiation in liquid precursors. Colloids and Surfaces A: Physicochemical and Engineering Aspects, 2013, 418, 47-51.	4.7	3
102	Superhydrophobic properties of cotton fabrics functionalized with ZnO by electroless deposition. Materials Chemistry and Physics, 2013, 138, 253-261.	4.0	62
103	Te and SiC co-doped MgB2 obtained by an ex situ spark plasma sintering technique. Scripta Materialia, 2013, 68, 428-431.	5.2	18
104	Antimicrobial activity of biopolymer–antibiotic thin films fabricated by advanced pulsed laser methods. Applied Surface Science, 2013, 278, 211-213.	6.1	14
105	MgB2 with Addition of Bi2O3 Obtained by Spark Plasma Sintering Technique. Journal of Superconductivity and Novel Magnetism, 2013, 26, 1553-1556.	1.8	5
106	Direct sintering of SiC–W composites with enhanced thermal conductivity. Fusion Engineering and Design, 2013, 88, 2598-2602.	1.9	13
107	Polymer Sphere Array Assisted ZnO Electroless Deposition. Soft Materials, 2013, 11, 457-464.	1.7	10
108	The genetics and neuropathology of neurodegenerative disorders: perspectives and implications for research and clinical practice. Acta Neuropathologica, 2012, 124, 297-303.	7.7	12

#	Article	IF	CITATIONS
109	Optical and electrical properties of arylenevinylene compounds thin films prepared by vacuum evaporation. Synthetic Metals, 2012, 161, 2612-2617.	3.9	7
110	Large scale microstructuring on silicon surface in air and liquid by femtosecond laser pulses. Applied Surface Science, 2012, 258, 9314-9317.	6.1	11
111	Sm3+-doped Sc2O3 polycrystalline ceramics: Spectroscopic investigation. Journal of Alloys and Compounds, 2012, 535, 78-82.	5.5	8
112	Luminescent micro- and nanofibers based on novel europium phthalate complex. Materials Chemistry and Physics, 2012, 136, 51-58.	4.0	2
113	Synthesis and characterization of bead-like particles based on chitosan and vinyl polymers. Journal of Polymer Research, 2012, 19, 1.	2.4	9
114	ZnO morphological, structural and optical properties control by electrodeposition potential sweep rate. Materials Chemistry and Physics, 2012, 134, 988-993.	4.0	13
115	Enhancement of critical current density and irreversibility field by Te or TeO2 addition to MgB2 bulk processed by spark plasma sintering. Scripta Materialia, 2012, 66, 570-573.	5.2	20
116	Synthesis of CdS nanostructures using template-assisted ammonia-free chemical bath deposition. Journal of Physics and Chemistry of Solids, 2012, 73, 1082-1089.	4.0	4
117	MgB2 with addition of Sb2O3 obtained by spark plasma sintering technique. Journal of Materials Science, 2012, 47, 3828-3836.	3.7	15
118	Spectroscopic characteristics of Dy3+ doped Y3Al5O12 transparent ceramics. Journal of Applied Physics, 2011, 110, .	2.5	60
119	Luminescent Dye-Doped KAP Nanorods Obtained by Template Assisted Crystallization. Journal of Nanoscience and Nanotechnology, 2011, 11, 3943-3948.	0.9	3
120	One Hundred Years since the Discovery of the "Umami―Taste from Seaweed Broth by Kikunae Ikeda, who Transcended his Time. Chemistry - an Asian Journal, 2011, 6, 1659-1663.	3.3	20
121	Effect of aqueous comonomer solubility on the surfactant-free emulsion copolymerization of methyl methacrylate. Journal of Polymer Research, 2011, 18, 25-30.	2.4	14
122	Hydrogen Generation from Photocatalytic Silver Zinc Oxide Nanowires: Towards Multifunctional Multisegmented Nanowire Devices. Small, 2011, 7, 2709-2713.	10.0	24
123	Substrate–target distance dependence of structural and optical properties in case of Pb(Zr,Ti)O3 films obtained by pulsed laser deposition. Applied Surface Science, 2011, 257, 5938-5943.	6.1	36
124	Temperature-dependent refractive index of potassium acid phthalate (KAP) in the visible and near-infrared. Optical Materials, 2011, 33, 812-816.	3.6	6
125	Intensity parameters of Tm3+ doped Sc2O3 transparent ceramic laser material. Optical Materials, 2011, 33, 501-505.	3.6	16
126	Polymer-assisted crystallization of low-dimensional lead sulfide particles. Physica E: Low-Dimensional Systems and Nanostructures, 2011, 43, 1826-1832.	2.7	2

#	Article	IF	CITATIONS
127	Silicon structuring by etching with liquid chlorine and fluorine precursors using femtosecond laser pulses. Journal of Applied Physics, 2011, 110, 034901.	2.5	19
128	Synthesis and properties of poly(methyl methacrylate-2-acrylamido-2-methylpropane sulfonic acid)/PbS hybrid composite. Materials Research Bulletin, 2010, 45, 1008-1012.	5.2	16
129	Luminescence of dye-doped KAP and KDP nanorods. Radiation Measurements, 2010, 45, 602-604.	1.4	4
130	Morphological and optical properties of doped potassium hydrogen phthalate crystals. Physica B: Condensed Matter, 2010, 405, 3722-3727.	2.7	32
131	Growth and optical characteristics of coumarin 6 doped potassium hydrogen phthalate (KAP) crystals. Optical Materials, 2009, 32, 281-285.	3.6	31
132	Influence of polyvinylpyrolidone as an additive in electrochemical preparation of ZnO nanowires and nanostructured thin films. Surface and Interface Analysis, 2008, 40, 556-560.	1.8	5
133	Optical spectroscopy of Yb2+ ions in YbF3-doped CaF2 crystals. Journal of Crystal Growth, 2008, 310, 2026-2032.	1.5	26
134	Transport properties of electrodeposited ZnO nanowires. Physica E: Low-Dimensional Systems and Nanostructures, 2008, 40, 2504-2507.	2.7	20
135	Electrical properties of electrodeposited CdS nanowires. Physica E: Low-Dimensional Systems and Nanostructures, 2008, 40, 2485-2488.	2.7	19
136	Functional Outcomes Can Vary by Dose: Learning-Based Sensorimotor Training for Patients Stable Poststroke. Neurorehabilitation and Neural Repair, 2008, 22, 494-504.	2.9	78
137	Preparation and Properties of Transition Metal Doped ZnO Nanowires. ECS Transactions, 2008, 16, 41-46.	0.5	8
138	Unwitting distributed genetic programming via asynchronous JavaScript and XML. , 2007, , .		30
139	Influence of geometrical properties on light emission of ZnO nanowires. Optical Materials, 2007, 30, 72-75.	3.6	13
140	Fractal characteristics of metal clusters self-assembled in alkali halide matrices. Physica Status Solidi C: Current Topics in Solid State Physics, 2007, 4, 727-731.	0.8	0
141	Tin nanoclusters obtained in potassium chloride by thermal annealing. Physica Status Solidi C: Current Topics in Solid State Physics, 2007, 4, 732-735.	0.8	Ο
142	Deposition and properties of CdTe nanowires prepared by template replication. Physica Status Solidi (B): Basic Research, 2007, 244, 1607-1611.	1.5	12
143	SiO x -P2O5 films—promising components in photonic structure. Optical and Quantum Electronics, 2007, 39, 511-521.	3.3	15
144	Heavy ion induced damage in NaCl and KCl crystals. Nuclear Instruments & Methods in Physics Research B, 2005, 229, 397-405.	1.4	14

9

#	Article	IF	CITATIONS
145	Silver nanoclusters in potassium halides obtained from Agâ^'-ions by electron detachment. Nuclear Instruments & Methods in Physics Research B, 2002, 191, 433-436.	1.4	3
146	A Model for Structures Growth by Sodium Electrodiffusion in Quartz Crystals. Crystal Research and Technology, 2002, 37, 868.	1.3	3
147	Fractal patterns formed by thermal treatment in alkali halide crystals. Physica B: Condensed Matter, 2002, 324, 387-392.	2.7	4
148	Optical absorption of Agâ^' centres in KCI:. Physica B: Condensed Matter, 2000, 275, 336-343.	2.7	4